TRANSIENT WAVE PROPAGATION IN LINEAR ACCELERATORS

J. Abraham
Argonne National Laboratory
Argonne, Illinois

Transients due to beam loading and other perturbations occurring in linear accelerators degrade the performance to the extent that it becomes necessary to correct for them in order to maintain satisfactory operation. Since the structure is large and the response time is long for such high Q systems, the question arises: Is it possible to correct the field amplitude and phase before the beam leaves the cavity? The answer depends on (a) the beam pulse durations and (b) the velocity with which energy propagates in the cavity. This paper is concerned with the determination of the velocity from observations made on the 50 MeV proton linac (Alvarez structure) at Argonne National Laboratory. For the purpose of analysis, it is assumed that the steady state condition obtains when the amplitudes of the forward and backward traveling waves are equal and, furthermore, that all transient can be explained in terms of these waves. Specifically, when a transient occurs, the forward and backward wave are unequal and the envelope of the disturbance is the output of our detector.

The transient response of the cavity to a step function input of the driving generator reveals the manner in which the energy builds up in the cavity. Since the structure is large (22.0 wavelengths), we are dealing with finite travel times of wave-fronts traveling back and forth in the cavity. These transient waves are best considered by the well known methods of microwave circuit theory[1, 2] wherein we consider only the transverse components of the waves; i.e., those components which give rise to the Poynting vector. More specifically, we need consider only the transverse electric field component of the Poynting vector from which the transverse magnetic field can always be determined from the relation $E_r / H_\theta = Z_0$ where Z_0 is the wave impedance in the guide.

Consider an arbitrary port (or terminal pair) in a wave guide system as shown in Fig. 1, where we define a normalized incident wave a_p, a complex scalar proportional to the complex magnitude of the transverse E-wave, E^+. Similarly, let b_p represent the normalized reflected or scattered wave, the complex magnitude of which is proportional to that of the reflected transverse E-wave, E_t^-. It is assumed that the waves a_p and b_p are normalized[3] such that

$$1/2\, a_p a_p = 1/2 \left| a_p \right|^2 = P_i \tag{1}$$

and

$$1/2\, b_p b_p^* = 1/2 \left| b_p \right|^2 = P_r \tag{2}$$

where P_i and P_r are the incident and reflected power at port p. It should be noted further that if port p is one port of a multiport network, then the reflected wave b_p will be a function of the inputs to all the other ports of the network in addition to that of port p so that

$$b_p = \sum_{q=1}^{n} s_{pq} a_p \tag{3}$$

where s_{pq} is the scattering coefficient. For a single port, however, a_p and b_p are related by

$$b_p = \Gamma_p a_p,$$

where Γ_p is the reflection coefficient of port p.

Equation 3 may be expanded for each port to give n simultaneous equations,

$$b_1 = s_{11}a_1 + s_{12}a_2 + \ldots\ldots\ldots\ldots + s_{1n}a_n$$

$$b_2 = s_{21}a_1 + s_{22}a_2 + \ldots\ldots\ldots\ldots + s_{2n}a_n$$

$$b_n = s_{n1}a_1 + s_{n2}a_2 + \ldots\ldots\ldots\ldots + s_{nn}a_n \tag{5}$$

or in matrix form

Work performed under the auspices of the U.S. Atomic Energy Commission

$$\begin{vmatrix} b_1 \\ b_2 \\ \vdots \\ b_n \end{vmatrix} = \begin{vmatrix} s_{11} & s_{12} & \cdots & s_{1n} \\ s_{21} & s_{22} & \cdots & s_{2n} \\ \vdots & \vdots & & \vdots \\ s_{n1} & s_{n2} & \cdots & s_{nn} \end{vmatrix} \begin{vmatrix} a_1 \\ a_2 \\ \vdots \\ a_n \end{vmatrix} . \tag{6}$$

In symbolic form, Eqn 6 is written,

$$\bar{b} = [S]\,\bar{a}$$

where $\bar{b}$ is a column vector representing the reflected or "scattered" output waves, $\bar{a}$ is the column vector representing the incident waves to the n ports, and $[S]$ is the scattering matrix of the network.

The specific network to be considered in this analysis consists of a center fed linac cavity and its waveguide feed line, both of which are assumed to be lossless (or, losses are negligible) and the cavity is assumed to be unloaded. Furthermore, the cavity will be treated as a cylindrical waveguide operating in a single mode, the $TM_{0,1}$ both ends being terminated in a short circuit. The network is shown in Fig. 2 where three reference planes are indicated by dashed lines to form a microwave T-junction. The junction is lossless and symmetrical so that waves incident on port three are divided equally between ports one and two. Futhermore, the junction is symmetrical about a reflection plane indicated by the dashed line P-P' so that it can be considered a Shunt (or H-plane) T-junction so that all the[4] properties of a shunt T-junction apply here. In the particular linac considered here (Argonne National Laboratory), the drive line represented by port three is a coaxial transmission line terminated in a magnetic loop. This configuration exhibits the same properties of symmetry as the shunt T-junction.

The junction may be represented analytically by a 3 x 3 scattering matrix which is given in its most general form by,

$$[S] = \begin{vmatrix} s_{11} & s_{12} & s_{13} \\ s_{21} & s_{22} & s_{23} \\ s_{31} & s_{32} & s_{33} \end{vmatrix} \tag{8}$$

for an isotropic medium. If the junction is lossless and the medium isotropic, then,

$$[S]^* [S] = [S]^{-1} [S] = [I] \tag{9}$$

where $[S]^*$ is the complex conjugate, $[S]^{-1}$ is the inverse matrix, and $[I]$ is the unitary matrix. Since the junction has reflection symmetry about the plane P-P', we can apply a matrix operator, called the "symmetry"[5] operator, which describes the reflection symmetry of the junction. The reflection operator, $[G]$ implies the symmetry of Maxwell's equations and is used here to obtain a reduced scattering matrix for the junction. Thus, from microwave network theory,

$$[S] = [G]\,[S]\,[G] \tag{10}$$

where $[G]$ is real, orthogonal, and unitary and has the form,

$$[G] = \begin{vmatrix} 0 & 1 & 0 \\ 1 & 0 & 0 \\ 0 & 0 & 1 \end{vmatrix} \tag{11}$$

for the shunt T-junction. When expanded, eqn. 10 becomes,

$$[S] = \begin{vmatrix} s_{22} & s_{12} & s_{23} \\ s_{12} & s_{11} & s_{13} \\ s_{23} & s_{13} & s_{33} \end{vmatrix} \tag{12}$$

so that,

$$s_{11} = s_{22} = \alpha$$
$$s_{13} = s_{23} = \gamma$$
$$s_{33} = \beta$$
$$s_{12} = \delta$$

and the reduced scattering matrix becomes,

$$[S] = \begin{vmatrix} \alpha & \delta & \gamma \\ \delta & \alpha & \gamma \\ \gamma & \gamma & \beta \end{vmatrix} \tag{13}$$

which has four variables instead of the orginal nine scattering coefficients. Since the junction is lossless, additional relationships exist among these four coefficients which can be obtained from the unitary property of $[S]$; i.e. $[S]\,[S]^* = 1$. The principal terms of interest are,

$$\begin{aligned} &(1,1) \text{ term of } [S]\,[S]^* = |\alpha|^2 + |\gamma|^2 + |\delta|^2 = 1 \\ &(3,3) \text{ term of } [S]\,[S]^* = |\beta|^2 + 2\,|\gamma|^2 = 1 \end{aligned} \tag{14}$$

The coefficients α, β, γ, and δ are intrinsic properties of the junction; however, by changing the reference plane at port 3, we can obtain β and γ in quadrature so that

$$\gamma = \pm \frac{j}{\sqrt{2}} \sqrt{1 - \beta^2} \tag{15}$$

which is consistent with eqn. 14. Reference planes 1 and 2 are chosen to be symmetrical at the voltage maxima in guides 1 and 2. The reflected waves at each reference plane of the junction can be expressed in terms of the incident waves appearing at all three reference planes as follows,

$$b_1 = \alpha a_1 + \delta a_2 + \gamma a_3 \tag{16}$$

$$b_2 = \delta a_1 + \alpha a_2 + \gamma a_3 \tag{17}$$

$$b_3 = \gamma a_1 + \gamma a_2 + \beta a_3 \tag{18}$$

Let the electrical length of the guide in arm 1 be $\phi/2$ radians from port 1 to the terminating short and the corresponding attenuation $\sigma/2$ nepers, as shown in Figure 3. The same length and attenuation are assumed for arm 2. Then $a_1 = -b_1 e^{-(\sigma+j\phi)}$ and $a_2 = -b_2 e^{-(\sigma+j\phi)}$. Furthermore, since the system is symmetrical, $|a_1| = |a_2|$ and $|b_1| = |b_2|$ the only difference being that, a_1 and a_2 travel in opposite directions, away from the junction simultaneously and similarly for b_1 and b_2. Then eqns. 16 and 18 become, if we assign negative values to the s_{11}, s_{12}, s_{22}, and s_{33} coefficients,

$$\begin{vmatrix} b_1 \\ b_2 \\ b_3 \end{vmatrix} = \begin{vmatrix} -\alpha & -\delta & jk \\ -\delta & -\alpha & jk \\ jk & jk & -\beta \end{vmatrix} \begin{vmatrix} -b_1 e^{-(\sigma+j\phi)} \\ -b_2 e^{-(\sigma+j\phi)} \\ a_3 \end{vmatrix} \tag{19}$$

where, α, δ, β, and k are real and positive, and $k = \left|\sqrt{\frac{1-\beta^2}{2}}\right|$.

The outgoing waves in arms 1 and 2 can be given in terms of the input wave to port 3, the drive line, and are:

$$b_1 = b_2 = \frac{jka_3}{\left[1 - |(\alpha+\delta)|\, e^{-(\sigma+j\phi)}\right]}, \tag{20}$$

$$b_3 = \left[\frac{+2k^2 e^{-(\sigma+j\phi)}}{\left[1 - |\alpha+\delta|\, e^{-(\sigma+j\phi)}\right]} - \beta\right] a_3 \tag{21}$$

For a given total attenuation and coupling, b_1, and b_2 will be a maximum for

$\phi = n\pi$, $n = 0, 1, 2, \ldots\ldots$

whereas, b_3 will be minimum. This is the condition of resonance, i.e., b_1 and b_2, the waves inside the cavity approach a maximum value, while b_3, the "reflected" wave in the waveguide becomes a minimum when the electrical length of the cavity is an integral number of half-wavelengths. With this value of ϕ, Eqns. 20 and 21 become,

$$b_1 = \frac{jka_3}{\left[1 - |\alpha+\delta|\, e^{-\sigma}\right]} = b_2, \tag{22}$$

$$b_3 = \left[\frac{2k^2 e^{-\sigma}}{\left[1 - |\alpha+\delta|\, e^{-\sigma}\right]} - \beta\right] a_3 \tag{23}$$

for the steady state condition at resonance.

The transient response of the cavity can be obtained by considering the forward wave in either arm 1 or 2 in this system, taking into account the wave velocity and successive reflections of the wave fronts. In addition, the leakage of waves in arm 1 to arms 2 and 3, and vice versa, must be taken into account which adds to the complexity. Nevertheless, the simplicity of the scattering matrix makes it possible to calculate the response readily. Assume a step function input of the wave a_3, in arm 3 at time $t = 0$. At this instant, waves of amplitude γa_3 travel to the right and left in arms 1 and 2, respectively. The waves a_1 and a_2 are both zero since the step has not yet reached the terminating short in these arms. After a time $t = T_1 = L/2v_e$, where L is the cavity length, and v_e is the velocity of the wave, a_1 jumps to the value $-b_1 e^{-\sigma}$, and, similarly, a_2 at port 2 jumps to the value $-b_2 e^{-\sigma}$ at the same instant. Designating the first transit of the input wave by the superscript "0", we have then, at $t \geq 0$:

$$b_1^0 = -\alpha a_1^0 - \delta a_2^0 + \gamma a_3 = \gamma a_3 \text{ since } a_1^0 = a_2^0 = 0.$$

At $t = T_1$, $a_1^1 = a_2^1 = -b_1^0 e^{-\sigma} = -\gamma a_3 e^{-\sigma}$,

$$b_1^1 = -\alpha a_1^1 - \delta a_2^1 + \gamma a_3 = (a+\delta)\gamma a_3 e^{-\sigma} + \gamma a_3$$

or

$$b_1^1 = \left[1 + (\alpha+\delta)e^{-\sigma}\right]\gamma a_3$$

i.e., they add up in phase because of the chosen reference plane at port 1 and because the wave a_3 due to the generator is constant. This value will be maintained for as long as the generator is in operation. This new step again travels to the right in arm 1, is attenuated and returns as $a_1^{(2)} = -b_1^{(1)} e^{-\sigma}$ so that, at $t = T_2(=T_1)$.

$$b_1^{(2)} = -\alpha a_1^{(2)} - \delta a_2^{(2)} + \gamma a_3$$

$$\text{or } b_1^{(2)} = (\alpha + \delta)e^{-\sigma}\left[1 + (\alpha + \delta)e^{-\sigma}\right]\gamma a_3 + \gamma a_3$$

$$= \gamma a_3 \left[1 + (\alpha + \delta)e^{-\sigma} + (\alpha + \delta)^2 e^{-2\sigma}\right]$$

Similarly, at $t = T_3(=T_1)$, $b_1^{(3)}$ becomes,

$$b_1^{(3)} = \gamma a_3 \left[1 + (\alpha + \delta)e^{-\sigma} + (\alpha + \delta)^2 e^{-\sigma} + + (\alpha + \delta)^3 e^{-3\sigma}\right]$$

and, for the nth transit of the wave b_1, we have

$$b_1^{(n)} = \gamma a_3\left[1 + (\alpha + \delta)e^{-\sigma} + (\alpha + \delta)^2 e^{-2\sigma} + \ldots\ldots + (\alpha + \delta)^n e^{-n\sigma}\right]. \tag{24}$$

Eqn. 24 is a geometric progression, the sum of the first n terms being,

$$s = \frac{a(1 - r^n)}{(1 - r)}.$$

If $\delta = b_1$, $a = \gamma a_3$, $r = (\alpha + \delta)e^{-\sigma}$, then, Eqn. 24 becomes,

$$b_1 = \gamma a_3 \left[\frac{1 - (\alpha + \delta)^n e^{-n\sigma}}{1 - (\alpha + \delta)e^{-\sigma}}\right] \tag{25}$$

Substituting the previously, assigned value of $\gamma = jk$, Eqn. 25 becomes

$$b_1 = jka_3 \left[\frac{1 - (\alpha + \delta)^n e^{-n\sigma}}{1 - (\alpha + \delta)e^{-\sigma}}\right] \tag{26}$$

Note that as $n \to \infty$, Eqn. 26 becomes Eqn. 20, the steady state value, as it should. When plotted as a function of the step number n, Eqn. 26, the envelope of b_1 has the appearance of an "escalator" as shown in Fig. 4.

Next, consider the transient that occurs at the end of a pulse when the generator is turned off. Consider b_3, the outgoing wave in the drive line. The steady state value is,

$$b_3 = \left[\frac{2k^2 e^{-\sigma}}{1 - (\alpha + \delta)\ e^{-\sigma}} - \beta\right] a_3 \tag{23}$$

At time $t = 0^+$, let the input a_3, collapse instantaneously to zero, then,

$$b_3^0 = \frac{2k^2 e^{-\sigma}}{1 - |(\alpha + \delta)|\ e^{-\sigma}}\ a_3 = B_3,$$

which is a small fraction of the huge wave traveling back and forth inside the cavity intercepted by the coupling. This value will be maintained for as long as it takes the waves inside to travel to both ends, be reflected, and return to the coupling with a negative going step since the waves inside are no longer being replenished. The value of $b_3^{(0)} = B_3$ at $t = 0$ is due to the incident waves at ports 1 and 2, which are $a_1^0 = A_1$, and $a_2^0 = A_2$.

That is,

$$b_3^0 = +jk(a_1^0 + a_2^0) = +j2kA_1 = B_3 \tag{24}$$

since $a_1^0 = a_2^0$ because of symmetry. These incident waves, a_1^0 and a_2^0 are reflected by the scattering coefficients $(s_{11} = s_{22} = -\alpha)$ and propagate to the right and left, respectively. Also traveling to the right (in arm 1), is the leakage from arm 2, $(-\delta a_2^0)$, while, the leakage from arm 1, $(-\delta a_1^0)$ travels to the left in arm 2 to form b_1^0 and b_2^0, respectively. Thus, since the leakage and reflected components in each arm add in phase, in arm 1, we have

$$b_1^0 = -\alpha a_1^0 - \delta a_2^0 = -(\alpha + \delta)a_1^0$$

which is the value of b_2^0 the only difference being in the direction of travel. These waves suffer an attenuation $e^{-\sigma}$ and a reflection at the terminating short, and after a travel time T_1, arrive at ports 1 and 2 as,

$$a_1^1 = -b_1^0 e^{-\sigma} = (\alpha + \delta)e^{-\sigma} A_1 = a_2^1.$$

This step couples out to arm 3 as,

$$b_3^1 = +jk(a_1^1 + a_2^1) = +j2k(\alpha + \delta)e^{-\sigma}A_1$$

so that, from Eqn. 24,

$$b_3^1 = (\alpha + \delta)e^{-\sigma}B_3.$$

The "new" waves a_1^1 and a_2^1 repeat this process, so that in arm 1, we have,

$$b_1^2 = -\alpha a_1^1 - \delta a_2^1 = -(\alpha + \delta)^2 a_1^1 = -(\alpha + \delta)^2 A_1$$

and similarly for arm 2. This results in a "new" incident wave at port 1 given by,

$$a_1^2 = -b_1^2 e^{-\sigma} = (\alpha + \delta)^2 e^{-2\sigma} A_1$$

which, in turn, produces another step in arm 3 as,

$$b_3^2 = +j2k(\alpha + \delta)^2 e^{-2\sigma} A_1 = (\alpha + \delta)^2 e^{-2\sigma} B_3$$

so that, for n trips (forward and back) of the waves a_1 and a_{2_1} we obtain,

$$b_3^n = (\alpha + \delta)^n e^{-n\sigma} B_3. \tag{27}$$

Eqn. 27 is another escalator function when plotted as a function of the step number n for integer values of n only, as shown in Fig. 5.

The step phenomena occurring at the leading and trailing edge of the cavity pulse are not usually observable, due to the bandwidth limitations of envelope detectors, and cavities are usually small in size, the linear accelerator being a notable exception. However, for a long cavity operating at, or near its dominant (waveguide) mode, the group velocity will be very small resulting in a long transit time for the internal waves. These conditions do prevail in the linear accelerator, so that the steps are readily observable with detectors having ordinary bandwidths. If we can measure the travel time accurately from one point to another in the cavity, then we can compute the group velocity which is the velocity with which energy propagates within the structure. This can be done easily by observing the detected output of a magnetic pickup loop in the cavity on an oscilloscope.

These observations have been made on the Argonne Linac, which is a 50 MeV machine used as the injector for the ZGS. However, since the linear accelerator is a loaded structure, we must define the velocity differently from that of an empty cavity. Since the purpose of loading in the linear accelerator is to reduce the phase velocity such that a point of constant phase will travel with the speed of the accelerated particle, $v_p \leq c$. The usual relation between the phase and group velocities is, $v_g v_p = c^2$, so that $v_g > c$ which implies that energy propagates faster than the speed of light in a loaded structure* which is impossible. We must conclude that v_g in a periodic structure is the group velocity; i.e.. the velocity of a wave packet, but not necessarily the velocity of energy propagation.[6] Instead, we define v_e the velocity of energy transport, which is given by,[7]

$$v_e = \frac{\bar{s}}{w} \tag{28}$$

where $\bar{s}$ is the Poynting vector and w is the energy density.

Observations made in the cavity are difficult to interpret since they are made using probes which couple to the magnetic field of the cavity, and the probes respond to a_1 and b_1, that is, the instantaneous sum of a_1 and b_1 in arm 1. Therefore, since the phase angles of the waves ($\phi = \beta z$) is a function of the position at which they are observed, we obtain both destructive and constructive interference. At loop 48, located L/4 from the high energy end, where L is total length of the cavity, the destruction is almost complete, that is, the amplitude of the steps is very small as shown in Fig. 12.

The difficulties one encounters in interpreting the observed waveforms in arms 1 and 2 are largely nonexistent in arm 3, the waveguide feed line. The reason is that, in arm 3 there is a reflectometer which "reads" the reflected wave b_3 only which is shown in Fig. 6. The leading edge has large oscillations due to the reaction of the load on the generator. These interfering oscillations appear also on the cavity pulses (leading edges), therefore, we restrict the observations to the trailing edge only, when the generator is off. Fig. 7 is delayed to show the steady state (pulse "on") and the trailing edge only. The similarity between Fig. 7 and Fig. 5, the calculated value of b_3, is apparent,

*Phase velocity and group velocity are independent of one another in a loaded structure. See reference 6.

while the detailed "escalator" function can be observed in Fig. 8 where the sweep rate has been expanded to 20. μsec/division. A further expansion of the sweep (Fig. 9) to 5. μsec/division provides a measure of the travel time from the center of the cavity and back which is, evidently 7. μsec from which we can conclude that the one way transit time is 3.5. μsec which corresponds to a velocity of 4.71 meters/μsec, approximately 1/60 the speed of light. This assumes, of course, that the energy velocity is constant and independent of position (in the cavity) at which the observation is made. However, variations due to the loading are not readily apparent.

The character of the escalator pattern changes with position when observed in the cavity. For example, Fig. 10 is the output of Loop No. 11 (located about L/8 from the low energy end) and shows the steps about the same as those in the drive line, while Fig. 11 is obtained from loop no. 33 which is the closest to the center (L/2) of the cavity. In Fig. 11 the steps have no flat top as in Fig. 10 and are seen to have a rather steep slope, which is probably due to the phase relations between forward and backward waves at the center. The sweep speed in Figs. 10 and 11 is 20. μsec/division and the amplitudes are equal, .5 v/div.

An example of destructive interference is evident from loop no. 48 (see Fig. 12) which is located L/4 from the terminating short (end wall) at the high energy end of the cavity. Fig. 13 is from loop no. 17 located near the L/4 point from the opposite (low energy) end. The sweep speed is again 20. μsec/division and the amplitude is .5 v/division for Figs. 12 and 13.

The steps in the photographs do not have the steep leading edge predicted by the theory. Increasing the bandwidth of the detector did not change the slope so bandwidth limitation did not explain the shape.

The gradual slope observed may be due to the dispersion relation of the loading and its effect on the group velocity since the various frequency components of the step will travel with different velocities.

References

[1] Altman, J. L., "Microwave Circuits" D. Van-Nostrand Co., Inc., Princeton, N. J., 1964.

[2] Montgomery, C. G., Dicke, R. H., and Purcell, E. M., "Principles of Microwave Circuits", McGraw-Hill Book Co., Inc., New York, 1948.

[3] Altman, J. L., op. cit., p. 41.

[4] Altman, J. L., Ibid., p. 101

[5] Montgomery, C. G., et al, op. cit., p. 430.

[6] Ginzton, E. L., "Microwave Measurements", McGraw-Hill Book Co., Inc., New York, 1957, p. 214.

[7] Kraus, J. D., "Electromagnetics", McGraw-Hill Book Co., Inc., 1953, p. 373.

[8] Brillouin, L., "Wave Propagation and Group Velocity, Academic Press, New York, 1960.

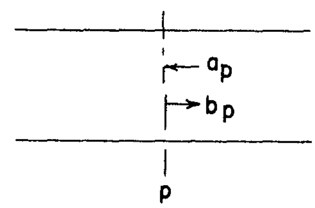

Fig. 1. Arbitrary port, or terminal pair in a waveguide system.

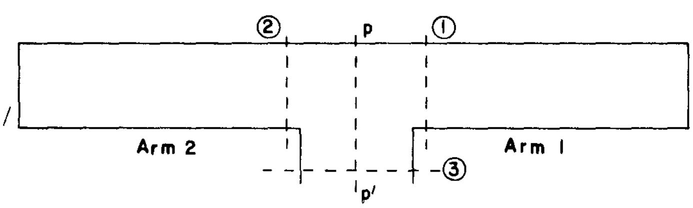

Fig. 2. Microwave network consisting of a center-fed cavity and waveguide feed line.

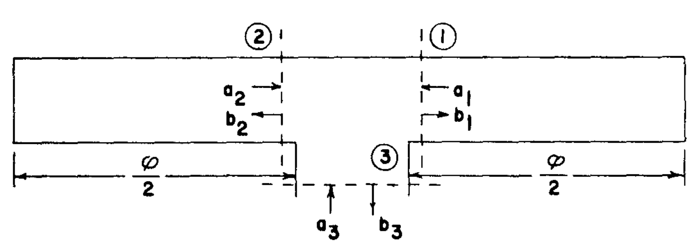

Fig. 3. Network indicating definition of terms in scattering matrix.

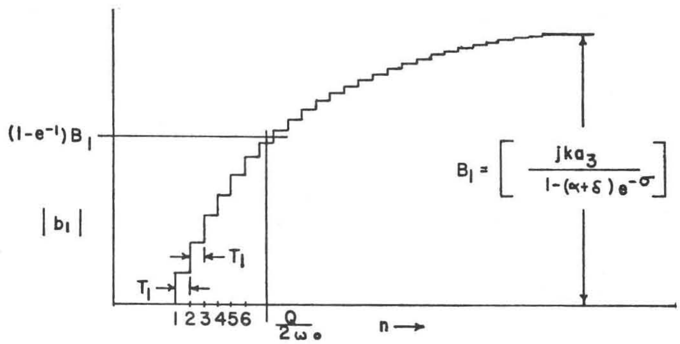

Fig. 4. Escalator function b_1 (Eq. 26).

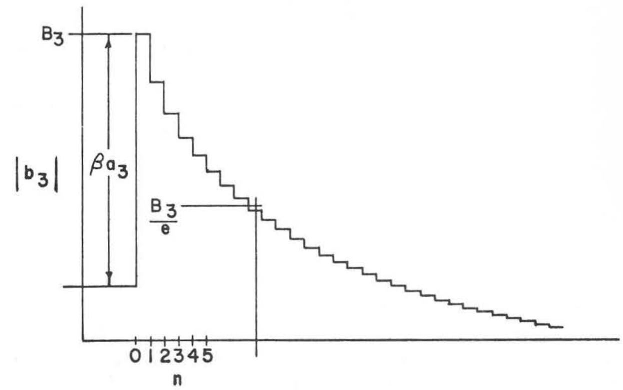

Fig. 5. Eq. 27, $b_3 = (\alpha + \delta)^n e^{-n\sigma} B_3$ vs step number n.

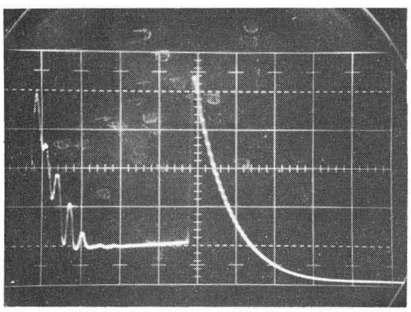

Fig. 6.

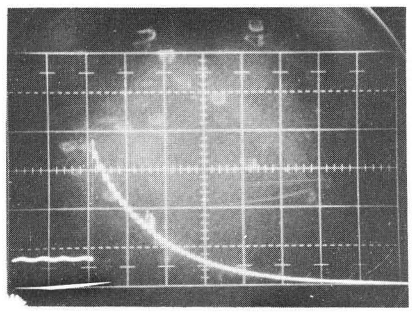

Fig. 7.

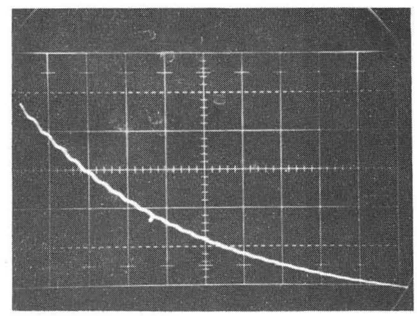

Fig. 8.

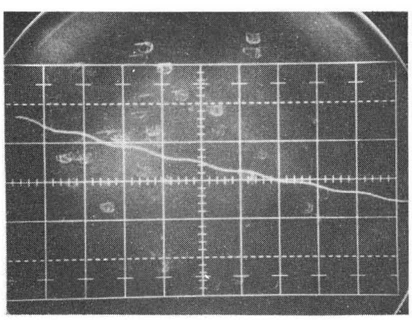

Fig. 9.

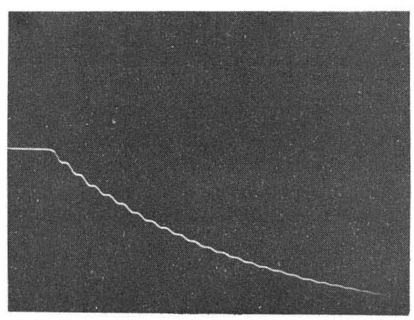

Fig. 10.

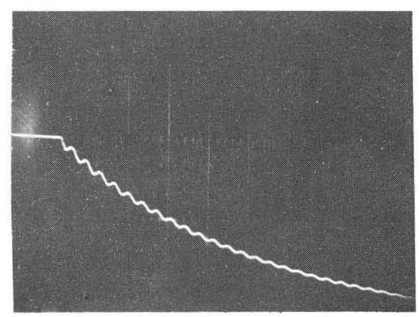

Fig. 11.

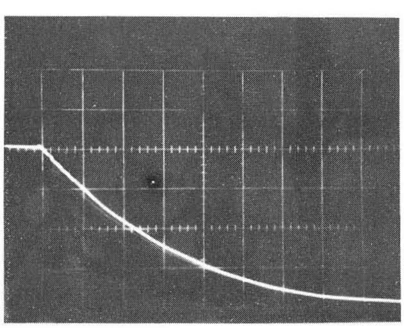

Fig. 12.

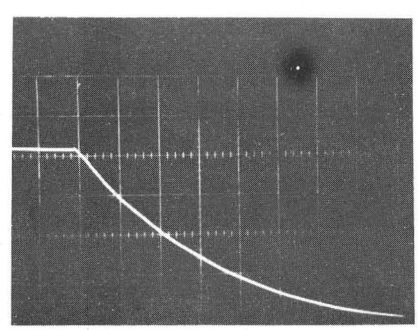

Fig. 13.